

---

# BALANCING EXPERT UTILIZATION IN MIXTURE-OF-EXPERTS LAYERS EMBEDDED IN CNNS

---

**Svetlana Pavlitskaya**

FZI Research Center for Information Technology  
76131 Karlsruhe, Germany  
pavlitskaya@fzi.de

**Christian Hubschneider**

FZI Research Center for Information Technology  
76131 Karlsruhe, Germany  
hubschneider@fzi.de

**Lukas Struppek\***

Department of Computer Science  
Technical University of Darmstadt  
64293 Darmstadt, Germany  
lukas.struppek@cs.tu-darmstadt.de

**J. Marius Zöllner**

FZI Research Center for Information Technology  
76131 Karlsruhe, Germany  
zoellner@fzi.de

April 25, 2022

## ABSTRACT

This work addresses the problem of unbalanced expert utilization in sparsely-gated Mixture of Expert (MoE) layers, embedded directly into convolutional neural networks. To enable a stable training process, we present both soft and hard constraint-based approaches. With hard constraints, the weights of certain experts are allowed to become zero, while soft constraints balance the contribution of experts with an additional auxiliary loss. As a result, soft constraints handle expert utilization better and support the expert specialization process, hard constraints mostly maintain generalized experts and increase the model performance for many applications. Our findings demonstrate that even with a single dataset and end-to-end training, experts can implicitly focus on individual sub-domains of the input space. Experts in the proposed models with MoE embeddings implicitly focus on distinct domains, even without suitable predefined datasets. As an example, experts trained for CIFAR-100 image classification specialize in recognizing different domains such as sea animals or flowers without previous data clustering. Experiments with RetinaNet and the COCO dataset further indicate that object detection experts can also specialize in detecting objects of distinct sizes.

## 1 Introduction

Mixture of experts (MoE) architectures, introduced in the early 1990s, rely on a set of expert models, each previously trained on a distinct domain or for a specific task. An additional model, the gating network, then decides input-dependent to what extent it relies on the individual expert predictions. Traditional MoE architectures using neural networks are trained in two separate steps: each expert individually, then the gating network. Furthermore, separate data sets for the experts are required. All experts perform partially redundant steps to extract information without a shared feature extractor. This costs valuable computing time, which is especially important in real-time applications such as autonomous driving or robotics. Sparsely-gated MoEs, embedded directly into the neural network layers, overcome these problems. However, under-utilization of distinct experts and a fixation on a small subset of experts used to prevent their direct application.

In this work, we insert MoE layers into convolutional neural networks (CNNs) and apply the approach to the basic computer vision tasks of image classification and object detection. All studied models with embeddings are trained end-to-end with standard optimizers and a single training set. We present various soft and hard constraints to tackle the problem of uneven expert utilization during training. The models further provide an additional hyperparameter to adjust

---

\*Work done while at Karlsruhe Institute of Technology (KIT).

the number of active experts in each forward pass and, thereby, the computational complexity. It allows us to train models with large capacity but, at the same time, maintain a beneficial computational complexity. Besides, embedded MoE layers enable us to interpret and gain insights into the decision-making process.

## 2 Related Work

Classic Mixture of Expert models, introduced by Jacobs et al. [1], contain a variable number of expert models and a single gating network to combine the expert outputs. These models do not support end-to-end training and require preliminary data clustering.

The concept of a sparsely-gated MoE layer by Shazeer et al. [2] combines the ideas behind MoEs and conditional computation [3] and integrates the MoE concept into a generic layer for neural networks. Unlike previous work on conditional computation for neural networks, the models with embedded MoE layers achieve remarkable results on language modeling and translation datasets with substantial model capacity improvements and minor computational efficiency losses. Unlike classic MoE approaches, sparse MoE layers form only a part of the entire model and are trained end-to-end with other network parts via backpropagation. The MoE layer activates experts only if their weights  $g_i(x)$  are non-zero to reduce computational complexity. It allows a network to have a large number of different experts in one layer to increase the model’s capacity and, at the same time, preserve sparse computations.

Recently, sparse MoEs have gained popularity for massive language models [2, 4]. Performance boosts, achieved via sparse MoEs, make training these models possible, although only on large clusters of powerful GPUs. In computer vision, the application of sparse MoE has centered around transformer models [5, 6, 7]. In contrast, in our work we consider CNNs, which is still the most widely spread architecture in the computer vision area.

### 2.1 Balancing expert utilization.

A known MoE problem is the focus of gating networks on a small subset of all available experts. The weights assigned to other experts are permanently zero or negligibly small. Because some experts start to perform better in the first iterations, the gating network increases their probabilities to be activated. Consequently, these few experts improve above average, and the gating network assigns even higher weights to them. This self-reinforcing process continues, s.t. the optimizer ends up in a local minimum [8].

Eigen et al. [8] propose a *hard constraint* on the relative gating assignments to each expert applied during training. For this, the weights assigned to each expert are summed over all training samples. If this value surpasses the average gating assignment by some threshold, the weights for the corresponding expert are set to zero. The remaining positive weights are then recomputed by a softmax function to maintain a convex combination of the experts.

Shazeer et al. [2] present a *soft constraint* approach introducing an auxiliary *importance loss*  $\mathcal{L}_{imp}$ . For this, the importance  $I_i(X)$  is defined as a sum of weights assigned to a particular expert  $E_i$  for a single batch  $X$ . The importance loss for batch  $X$  is then defined as  $\mathcal{L}_{imp} = w_{imp} \cdot CV(I(X))^2$ , where  $w_{imp}$  is a weighting factor and  $CV$  is the coefficient of variation.  $\mathcal{L}_{imp}$  encourages equal importance for all experts during training. The number of training samples per expert may still vary since importance is used instead of the mean number of samples per expert.

## 3 Constraints for Balancing Expert Utilization

We refer to the problem of unbalanced expert utilization in an MoE layer as *dying experts*, analogous to the dying ReLU problem [9]. We consider experts as dead, if they receive less than 1% average importance on the test set. To mitigate it, we propose two hard constraints and one soft constraint.

### 3.1 Probabilistic Definition of an MoE.

Formally, an MoE consists of a set of expert networks  $E$  with size  $|E| = N$  that contains expert models  $E_1, \dots, E_N$ . For a given input  $x$ , each expert  $E_i$  produces an output  $e_i(x)$ . The gating network  $G$  computes a weight vector  $G(x)$  with length  $N$  for the set of experts  $E$ . Inputs of experts and the gating network may differ. For simplicity, we assume that both inputs are identical. The gating network then applies a softmax function to turn its output logits  $H(x)$  into weights  $g_1(x), \dots, g_N(x)$  for  $N$  experts. The final MoE output is computed as a convex combination of the expert outputs.

We interpret an MoE model as a probability model in which class probabilities are marginalized over expert selection. Each weight  $g_i(x)$  can be seen as the probability  $p(E_i|x)$  to select a specific expert for a given input. Outputs of each

expert  $e_i(x)$  quantify the probability  $p(c|E_i, x)$  of each class  $c \in C$ . The MoE output is then defined as follows:

$$F_{MoE}(x) = \sum_{i=1}^N p(E_i|x)p(c|E_i, x) = p(c|x) \quad (1)$$

### 3.2 Hard constraints on importance.

Based on the work of Eigen et al. [8], we propose two hard constraints on importance. We define the relative importance  $I_i^{rel}(t)$  of expert  $E_i$  for batch  $X_t$  at time step  $t$  as follows:

$$I_i^{rel}(t) = \frac{I_i(X_t) - \mu_{I(X_t)}}{\mu_{I(X_t)}} = \frac{I_i(X_t) - \frac{|X_t|}{N}}{\frac{|X_t|}{N}} \quad (2)$$

The *relative importance constraint* is based on the running relative importance  $\sum_{t'=1}^t I_i^{rel}(t')$  of expert  $E_i$  at time step  $t$ . We set  $g_i(x) = 0$  for  $x \in X_{t+1}$  if  $\sum_{t'=1}^t I_i^{rel}(t') > m_{rel}$  for some threshold  $m_{rel}$ . Recent values have the most substantial impact on the constraint because we sum up relative importance values. Earlier relative importance values compensate each other or are compensated by exceeding the threshold  $m_{rel}$  and deactivating experts.

The *mean importance constraint* is based on the mean importance  $\bar{I}_i$  assigned to expert  $E_i$  up to time step  $t$ . Similar to the previous constraint, we set  $g_i(x) = 0$  for  $x \in X_{t+1}$  if  $\bar{I}_i(t) - \mu_{I(X_t)} > m_{mean}$  for some threshold  $m_{mean}$ . Whereas the relative importance constraint takes a stronger focus on the recent past, the mean importance approach takes a holistic view, with all past importance values having the same impact on the constraint.

Both hard constraints are only active during training and deactivate experts for an entire batch. In experiment, we observed a stabilization process of expert utilization in practice after a few training iterations and with a decreased learning rate. We further show that the constraint-based on relative importance manages expert utilization better than the mean importance constraint.

### 3.3 Soft constraint based on KL-divergence.

In addition to the auxiliary importance loss [2], we propose another soft constraint that takes a probabilistic view on expert importance. According to Equ. 1, we interpret the gating network output as a discrete probability distribution  $P$  with probability  $P(E_i|\mathcal{X})$  for expert  $E_i$  being selected for input  $\mathcal{X}$  (here  $\mathcal{X}$  is a random variable for input  $x$ ). In expectation, the gating network should assign each expert  $E_i$  the same average weighting, equal to  $\mathbb{E}_X[P(E_i|\mathcal{X})] = \frac{1}{N}$ . The expected weight assignment corresponds to a discrete uniform distribution  $Q$  with probability  $Q(E_i|\mathcal{X}) = Q(E_i) = \frac{1}{N}$ .

We define an auxiliary *KL divergence loss*  $\mathcal{L}_{KL}$  as the KL-divergence  $D_{KL}$  between  $P$  and  $Q$ , weighted by hyperparameter  $w_{KL}$ . The probability  $P(E_i|\mathcal{X} = X) = \frac{I_i(X)}{|X|}$  is computed as the average importance per sample in batch  $X$ .  $\mathcal{L}_{KL}$  is then defined as follows:

$$\mathcal{L}_{KL} = w_{KL} \cdot D_{KL}(P||Q) = w_{KL} \cdot \sum_{i=1}^N P(E_i|X) \cdot \ln \left( \frac{P(E_i|X)}{Q(E_i)} \right) \quad (3)$$

The loss functions reach their maximum if a single expert receives all the weights. The maximum value for  $\mathcal{L}_{imp}$  corresponds to the number of experts in the model. For  $\mathcal{L}_{KL}$ , the maximum value corresponds to the natural logarithm of the number of experts.

$\mathcal{L}_{imp}$  assigns larger values to an unequal importance distribution than  $\mathcal{L}_{KL}$ . The larger the inequality, the more the loss functions diverge from each other. Consequently,  $\mathcal{L}_{imp}$  penalizes inequality in importance distribution harder than  $\mathcal{L}_{KL}$ .  $\mathcal{L}_{imp}$  would be more useful if we aim to an equal expert utilization. However, we might want a higher variance in the expert utilization for some models but still avoid dying experts. In this case,  $\mathcal{L}_{KL}$  would be the better choice to allow for larger deviations from an equal importance distribution.

## 4 Experiments

In the following we evaluate the proposed soft and hard constraints for the embedded sparsely-gated MoE layers on two computer vision tasks: image classification and object detection.

### 4.1 Image Classification Enhancements with MoE Layers

In the first part of the experiments we evaluate embedding sparsely-gated MoE layers into ResNet-18 for image classification task on CIFAR-100 dataset. We replace distinct ResNet blocks with MoE layers using deep experts and analyze expert utilization for soft and hard constrained models. We further analyze the behavior of distinct experts and the per-class prediction accuracy of these.

#### 4.1.1 Dataset and Baseline.

Experiments are performed on the CIFAR-100 dataset [10] with the official train/test split. The baseline follows a ResNet-18 [11] architecture<sup>2</sup>. To match the input dimension of CIFAR-100, we reduce the filter size of the input layer to  $3 \times 3$  with stride 1 and remove max-pooling.

#### 4.1.2 Expert and Gate Architectures.

ResNet-18 consists of 4 blocks. The MoE experts follow the architecture of the ResNet blocks, but we adjust the number of filters of each expert in a bottleneck manner, thus reducing the number of parameters to maintain comparable computational complexity. The number of channels in each expert is the same as in the corresponding ResNet block. We also consider a slightly modified *Shortcut* MoE architecture with an additional projection shortcut that connects the MoE layer input with its output. MoE layers that are more deeply embedded in a model and have deeper expert networks will probably benefit from shortcuts similar to vanilla ResNets.

We consider two gate architectures: *SimpleGate* and *ConvGate*. The *SimpleGate* first applies global average pooling, reducing each feature map to a single value. The resulting values are then processed by a single fully connected layer with number of neurons corresponding to the number of experts. Weights are then calculated with a softmax function. The *ConvGate* adds a convolutional layer with  $3 \times 3$  filters.

#### 4.1.3 Single Layer MoE Embeddings.

We first replace the last convolutional layer in different ResNet-18 blocks with an MoE layer containing 4 experts, s.t. each model only contains a single MoE layer. The gating networks follows the *SimpleGate* architecture with  $k = 2$ . We set the weights for auxiliary losses to  $w_{imp} = w_{KL} = 0.5$ , thresholds for hard constraints to  $m_{rel} = 0.5$  and  $m_{mean} = 0.3$ . The models are referred to as *SingleMoE-Constraint-Position-NumExperts*, whereas the constraint is either *Imp*, *KL*, *Rel* or *Mean*. Position numbers refer to different ResNet blocks, whereas position 0 refers to the first convolutional layer, which directly processes the input image.

The results (see Table 1) show, that *KL*-models mostly perform better than *Imp*-models. Independently of the constraint, models with MoE layers in position 0 achieve the lowest test accuracy. The increased capacity and specialization using different experts thus do not benefit from the low-level feature processing.

The performance for MoE layers in the last position decreases for soft constrained, but increases for hard-constrained models. The equal importance between experts as pursued by both auxiliary loss functions is thus not beneficial. It seems to increase accuracy when models utilize some experts more often than others. High-level features probably cannot be divided efficiently into equally-sized groups, such that each expert is responsible for a similar number of features.

#### 4.1.4 Soft Constrained MoE Blocks.

Next, we replace one complete ResNet block with an MoE layer. All models are trained from scratch without pre-trained weights,  $w_{imp} = w_{KL} = 0.5$ . ResNet expert and *SimpleGate* architectures are used in the MoE layers with 4 and 10 experts,  $k = 2$  as above. We train models with 4 experts for 150 epochs and models with 10 experts for 180 epochs. Table 2 shows test results for basic and shortcut models. The models are denoted *MoE-Constraint-Position-NumExperts*.

<sup>2</sup>We use the official PyTorch implementation available at <https://github.com/pytorch/vision/blob/master/torchvision/models/resnet.py>

Table 1: Mean accuracy and sample standard deviation of *SingleMoE* models.  $<>$  stands for the corresponding constraint (see column names)

Model / Constraint	<i>Imp</i>	<i>KL</i>	<i>Rel</i>	<i>Mean</i>
<i>Baseline</i>	$72.62 \pm 0.29$			
<i>SingleMoE-&lt;&gt;-0-4</i>	$71.59 \pm 0.25$	$72.10 \pm 0.51$	<b><math>72.16 \pm 0.14</math></b>	$72.06 \pm 0.06$
<i>SingleMoE-&lt;&gt;-1-4</i>	$72.56 \pm 0.04$	<b><math>72.72 \pm 0.32</math></b>	$73.02 \pm 0.40$	$72.51 \pm 0.37$
<i>SingleMoE-&lt;&gt;-2-4</i>	$72.63 \pm 0.13$	<b><math>73.00 \pm 0.14</math></b>	$73.02 \pm 0.29$	$73.09 \pm 0.37$
<i>SingleMoE-&lt;&gt;-3-4</i>	<b><math>72.78 \pm 0.20</math></b>	$72.57 \pm 0.21$	$72.71 \pm 0.45$	$72.92 \pm 0.28$
<i>SingleMoE-&lt;&gt;-4-4</i>	$72.34 \pm 0.40$	$72.40 \pm 0.09$	<b><math>73.54 \pm 0.30</math></b>	$73.37 \pm 0.19$

Table 2: Mean accuracy and sample standard deviation of soft constrained *MoE* models.  $<>$  stands for the corresponding constraint (see column names)

Model / Constraint	<i>Imp</i>		<i>KL</i>	
	<i>Basic</i>	<i>Shortcut</i>	<i>Basic</i>	<i>Shortcut</i>
<i>Baseline</i>	$72.62 \pm 0.29$			
<i>MoE-&lt;&gt;-1-4</i>	$72.20 \pm 0.24$	$72.24 \pm 0.49$	$72.21 \pm 0.29$	<b><math>72.72 \pm 0.36</math></b>
<i>MoE-&lt;&gt;-1-10</i>	$70.94 \pm 0.14$	<b><math>71.51 \pm 0.23</math></b>	$70.76 \pm 0.48$	$71.32 \pm 0.60$
<i>MoE-&lt;&gt;-2-4</i>	$71.75 \pm 0.22$	$72.18 \pm 0.29$	$71.78 \pm 0.37$	<b><math>72.25 \pm 0.17</math></b>
<i>MoE-&lt;&gt;-2-10</i>	$70.71 \pm 0.25$	$72.76 \pm 0.50$	$70.63 \pm 0.44$	<b><math>71.87 \pm 0.30</math></b>
<i>MoE-&lt;&gt;-3-4</i>	$71.45 \pm 0.24$	<b><math>71.65 \pm 0.43</math></b>	$71.45 \pm 0.40$	$71.54 \pm 0.22$
<i>MoE-&lt;&gt;-3-10</i>	$70.72 \pm 0.30$	<b><math>71.47 \pm 0.29</math></b>	$70.88 \pm 0.20$	$71.43 \pm 0.12$
<i>MoE-&lt;&gt;-4-4</i>	$71.52 \pm 0.09$	<b><math>71.95 \pm 0.39</math></b>	$71.37 \pm 0.04$	$71.80 \pm 0.23$
<i>MoE-&lt;&gt;-4-10</i>	$70.70 \pm 0.30$	$71.61 \pm 0.16$	$71.16 \pm 0.40$	<b><math>71.99 \pm 0.23</math></b>

*Shortcut* MoE models always outperform equivalent basic models. The differences are especially drastic for models with 10 experts. Therefore, we only focus on models with shortcut connections in further experiments.

Furthermore, models with 4 experts almost always outperform models with 10 experts, although the latter offer a much larger capacity and theoretically enable each expert to specialize in a smaller domain. Evidently, models with MoE layers in lower positions do not benefit from an increased capacity because the range of low-level features is much smaller than for high-level features. Also, differences between models with 4 and 10 experts decrease the deeper we insert the MoE blocks. Another reason may be that each of the 10 experts only sees about half the number of samples during training compared to models with 4 experts. However, longer training does not help, because the model converges at some point and no further accuracy improvements are apparent in later epochs.

Both auxiliary losses deliver similar results. The only model that slightly beats the baseline is *MoE-KL-1-4 Shortcut*, performance differences are otherwise insignificant. Embeddings in lower positions lead to better performance than in higher positions. MoE blocks embedded in position 1 deliver the best performance. On the other hand, the worst evaluation results are achieved by models with embeddings in position 3. These results are consistent with our results using single layer experts above.

We further illustrate the effect of the soft constraints during the training process in Fig. 1. We measure expert utilization after each training epoch as the average assigned importance on the test set. The figures demonstrate that both loss functions handle expert utilization similarly, and further confirm that expert utilization varies less for MoE blocks in deeper positions.

We additionally analyze expert utilization for different model setups by computing the coefficient of variation *CV*. We classify an expert as alive if it receives at least 1% average weighting on the test set. Almost all models show full expert utilization with no dying experts. This demonstrates that both loss functions are generally able to overcome the dying expert problem. Detailed results on expert utilization are provided in the supplements.

#### 4.1.5 Hard constrained MoE blocks.

Next, we train models with relative and mean importance constraints. As mentioned above, we only train *Shortcut* models. We set  $m_{rel} = 0.5$  and  $m_{mean} = 0.3$ , equally to single layer MoE models.

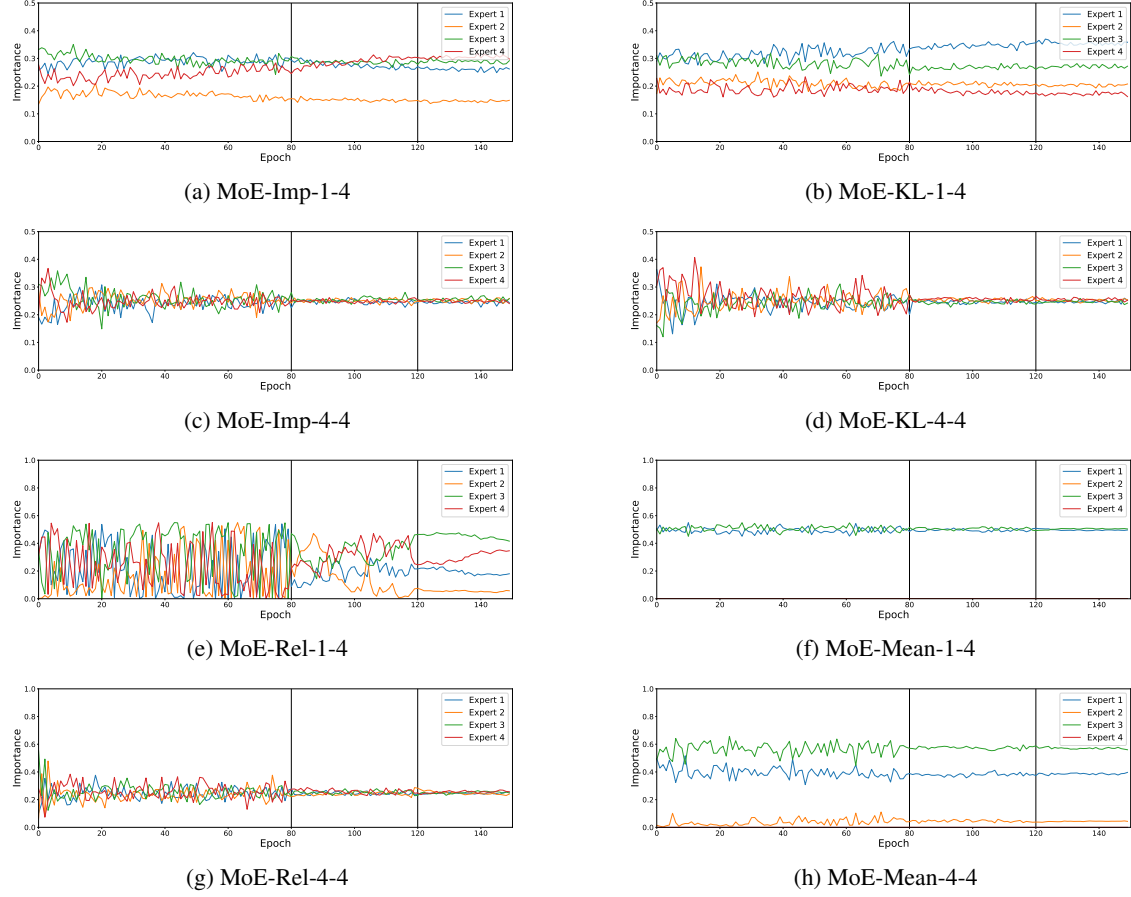


Figure 1: Average importance assignment on the test set over the training epochs for models trained with soft (a-d) and hard (e-h) constraints. Expert utilization is shown for the models with the best test accuracy. Black vertical lines denote learning rate decreases.

Table 3 shows experimental results. Most *Mean*-models overperform other models. While comparable soft constrained models show the best performances in positions 1 and 2, hard constrained models perform mostly better for embeddings in positions 1 and 4. Similar to soft constrained models, MoEs with 4 experts almost always beat models with 10 experts.

*Rel*-models models with 4 experts significantly beat the baseline for embeddings in position 4. Like soft constrained models, the lowest performances are achieved in position 3. We assume that embedded MoE blocks perform generally better for positions either early or late in a network.

We again plot the averagely assigned importance to each expert over training epochs for the test set in Fig. 1. For *Rel*-models, the effect of a decreasing learning rate is similar to soft constrained models and stabilizes expert utilization. *MoE-Rel-4-4* shows a robust training process, which stabilizes after the first few training epochs. *Mean*-models seem to be very stable during training. However, the models only keep 2 and 3 experts alive, respectively. The number of living experts and the tendency of assigned importance are determined in the first epochs and do not change until the end. It shows that accuracy achievements by mean importance constraints are due to the higher number of training samples each living expert receives.

We also analyze the expert utilization, detailed results are provided in the supplements. Both hard constraints have problems with dying experts. In particular, *Mean*-models are unable to keep all experts alive in a single model. Relative importance constraints manage to overcome the dying expert problem for models with 4 experts, but still face problems with 10 experts. Only *MoE-Rel-4-10* shows improvements in the number of living experts and keeps all experts alive.

Even in experiments with varying threshold values, *Mean*-models show large dying expert problems. When we also take expert utilization into account, the top performance by *Mean*-models is caused by using only a part of all available

Table 3: Mean accuracy and sample standard deviation of hard constrained *MoE* model.  $<>$  stands for the corresponding constraint (see column names)

Model / Constraint	<i>Rel</i>	<i>Mean</i>
<i>Baseline</i>	$72.62 \pm 0.29$	
<i>MoE-&lt;&gt;-1-4</i>	$72.21 \pm 0.42$	<b><math>73.00 \pm 0.40</math></b>
<i>MoE-&lt;&gt;-1-10</i>	$71.60 \pm 0.09$	<b><math>72.28 \pm 0.15</math></b>
<i>MoE-&lt;&gt;-2-4</i>	$72.18 \pm 0.48$	<b><math>72.95 \pm 0.35</math></b>
<i>MoE-&lt;&gt;-2-10</i>	$71.51 \pm 0.44$	<b><math>72.08 \pm 0.32</math></b>
<i>MoE-&lt;&gt;-3-4</i>	$72.05 \pm 0.15$	<b><math>72.61 \pm 0.37</math></b>
<i>MoE-&lt;&gt;-3-10</i>	$70.82 \pm 0.16$	<b><math>72.05 \pm 0.61</math></b>
<i>MoE-&lt;&gt;-4-4</i>	<b><math>73.10 \pm 0.25</math></b>	$72.57 \pm 0.31$
<i>MoE-&lt;&gt;-4-10</i>	$72.84 \pm 0.30$	<b><math>73.09 \pm 0.35</math></b>

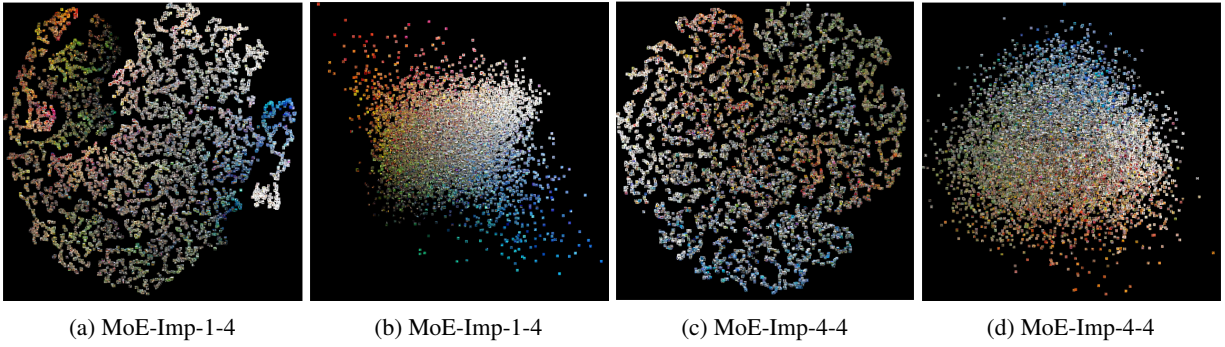


Figure 2: Visualization of gating network logits using t-SNE (a,c) and PCA (b,d)

experts. The reason for better performance is that a few experts are alive during training and consequently trained on a larger number of training samples than models with more experts alive.

Overall, *Rel*-models show significantly higher variations compared to soft constrained models. It demonstrates that their expert utilization varies much more, and some experts are activated more frequently than others. Since *Mean*-models perform significantly better than soft constrained models with embeddings in deeper positions, it seems beneficial to allow the expert importance to vary more during training instead of pushing importance to similar values by auxiliary losses. Since mean importance has significant problems with dying experts, we will exclude this constraint from some further experiments and focus on relative importance.

#### 4.1.6 Visualization of gating network decisions.

To understand, how gating networks make decisions and assign weight to distinct experts, we apply t-SNE and PCA to the raw gating network logits over the test set. Fig. 2 demonstrates visualizations exemplary for the shortcut models *MoE-Imp-1-4* and *MoE-Imp-4-4*. For *MoE-Imp-1-4*, gating networks close to the model input layer assign weights apparently mainly based on the dominant colors of input images. For *MoE-Imp-4-4*, the distinctions are much more faded. *KL*-models demonstrate similar results.

Fig. 3 shows the resulting sample assignment to different experts for two active experts per forward pass. *MoE-Imp-1-4* gate divides the data into 2 major subdomains, while *MoE-Imp-4-4* gate varies more widely between different expert combinations. Weight assignment in deeper MoE layers is therefore based more on high-level features leads to stronger differentiation between experts.

Detailed analysis of the t-SNE plots (see supplements) has confirmed, that the gating network in position 4 puts a stronger emphasis on high-level features and similar image classes. For hard constrained models, visible structures are less significant compared to the soft constrained model. Gating networks with 10 instead of 4 experts produce similar visual results for soft and hard constraints.

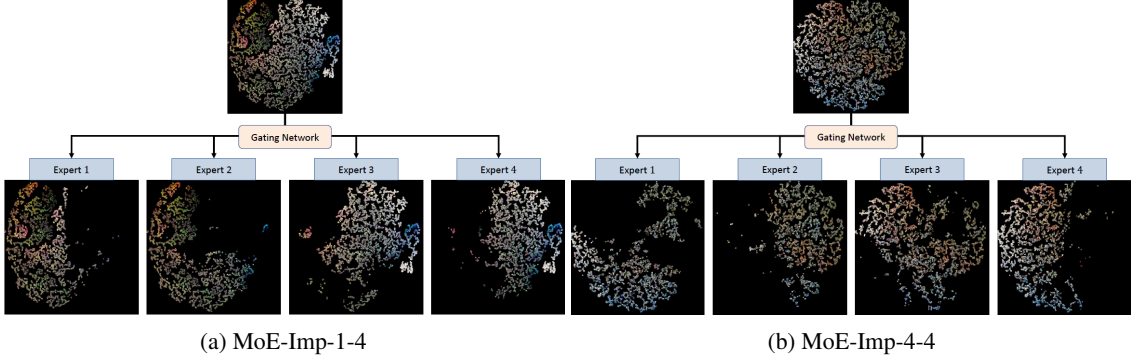


Figure 3: Assignment of input samples to specific experts in soft constrained models, visualized with t-SNE. The gating network in position 4 (b) shows a more diversified expert utilization compared to the gating network in position 1 (a)

#### 4.1.7 Prediction accuracy for distinct classes.

To examine the MoE behavior quantitatively, we compare the per-class accuracy for the baseline and MoE models with embeddings in positions 1 and 4. Complete class-wise test results are provided in the supplements.

The soft constrained models show improved performances for some groups of classes, which are difficult to distinguish for the baseline. In particular, *MoE-Imp-4-4* shows performance improvements for groups (*crab*, *lobster*) and (*maple tree*, *oak tree*, *willow tree*) and outperforms the baseline on these classes. The accuracy on the full test set is still almost 0.7% below the baselines. MoE thus helps to differentiate between these classes better, but at the cost of other class accuracies. *MoE-KL-1-4* significantly outperforms the baselines for group (*snake*, *worm*) and achieves comparable accuracy on the full test set.

For hard constrained models, *MoE-Rel-4-4* shows improvements for group (*beaver*, *shrew*, *mouse*) and also massive improvements for other classes like *leopard*, *lizard*, and *possum*. *MoE-Mean-1-4* shows significant accuracy improvements for the same group and other animals. Otherwise, no further clear improvements for the class pairs are notable. *MoE-Rel-4-4* and *MoE-Mean-1-4* outperform the baseline models by about 0.5%.

Overall, MoE models can in some cases better differentiate between similar classes than baseline models and consequently increase prediction accuracy for these specific classes. However, it comes at the cost of decreased prediction accuracy for other classes.

#### 4.1.8 Varying number of active experts.

We analyze the impact of the varying number of active experts  $k$ . For this, we evaluate on the test set the *Shortcut* models trained with  $k = 2$ , results are averaged for 3 runs. Detailed results are provided in the supplements.

The accuracy of most models increases for a larger number of active experts. Except for *Mean*-models, the best results are achieved with  $k = 3$ . This supports our assumption that experts in deeper positions learn more diversified high-level features and specialize in a more specific domain than experts in lower layers. Experts in positions 1 and 2 are all similarly able to extract meaningful low-level features. On the other hand, MoE blocks, embedded in deeper network positions, benefit from increasing the number of experts available. *MoE-Rel-4-4*, as the best performing model with 4 active experts, outperforms the baseline significantly by almost 1%.

Overall,  $k$  can be seen as a trade-off parameter between accuracy and computational complexity. Vanilla ResNet-18 networks reach 0.56 GMac and are comparable to models using  $k = 2$  experts. Each additionally activated expert thus adds about 0.06 to 0.08 GMac.

#### 4.1.9 Utilization of distinct experts.

To analyze the implicit specialization of experts on distinct subdomains of the input space, we only activate one specific expert during evaluation and assign all weights to it. We run these experiments exemplary for *MoE-Imp-4-4* and *MoE-Rel-4-4* since both models achieve the best performances for  $k = 4$  and do not suffer from dying experts.

The gating networks tends to select different experts for specific classes. We can roughly assign each expert to a subdomain of classes as follows: expert 1 – marine animals, vehicles, and outdoor scenes; expert 2 – different animals

ashore; expert 3 – flowers, fruits, and vegetables; expert 4 – furniture and household devices. Consequently, the MoE layer implicitly learned to create experts specialized in distinct subdomains. See supplements for detailed results.

#### 4.1.10 Improvements via *ConvGate*

We finally evaluate possible improvements via replacing *SimpleGate* with *ConvGate*, exemplary for *MoE-Imp-4-4*. After adjusting the learning rate schedule, *MoE-Imp-4-4* with *ConvGate* reaches the accuracy of  $72.42 \pm 0.27$ , beating the *SimpleGate* model, but not the baseline.

We take the best performing *ConvGate* model with Gaussian noise and compute again each distinct expert’s test accuracy and utilization. The class-wise results are provided in the supplements. Comparing results to MoE-Imp-4-4 using *SimpleGate*, the distinct experts in the *ConvGate* model perform about 4% worse on average. Still, the full MoE model achieves 72.70% overall accuracy compared to 72.39% for the best soft constrained model with *SimpleGate*.

Visualization of the assignments with t-SNE plots shows, that *ConvGate* subdivides the assignments much clearer (see supplements for details). Consequently, the gating network produces more unambiguous weight vectors and selects experts more definitely.

### 4.2 Object Detection Enhancements with MoE Layers

In the second part of the experiments, we evaluate embedding sparsely-gated MoE layers into *RetinaNet* for object detection task on COCO dataset.

#### 4.2.1 Dataset and Baseline.

We use COCO dataset [12] for the experiments: 2017 train and test-dev split. Metrics are computed on the 2017 validation set containing 5,000 images and also by uploading detection results onto an evaluation server. We use a pretrained *RetinaNet* [13] as a baseline. It uses *ResNet-50* backbone and an image scale of 600. We train all models using  $\gamma = 2$  and  $\alpha = 0.25$  for focal loss. All models are based on an unofficial PyTorch reimplementation for *RetinaNet*<sup>3</sup>. For all models, we report standard COCO metrics mAP@[.5, .95] and mAP@.5.

#### 4.2.2 MoE Embedded into Regressor and Classifier.

We replace the regression and classification subnets with 2 separate MoE blocks, referred to as *DetectorMoE*. The model is trained end-to-end, using the vanilla classification and regression subnets as expert networks. We only train models with 4 experts in each MoE layer and set  $k = 2$ .

We omit mean importance constraints due to previously observed dying expert problems. Weighting factors are reduced to  $w_{imp} = w_{KL} = 0.25$  to guarantee achieve better expert utilization for deeper MoE layers. Additionally, we set  $m_{rel} = 0.3$  to avoid dying experts. Each model uses pre-trained weights for the *ResNet-50* feature extractor. We keep those weights frozen during training to increase training speed and reduce GPU memory usage. We also train models with unfrozen weights but do not observe performance improvements. The gating network is *ConvGate*. All experts are initialized using Kaiming approach [14] to learn more diverse features compared to using pre-trained weights.

In addition to models with 2 separate gating networks, we also train one MoE model (denoted as *Single*) with a single gating network shared between regressor and classifier MoE blocks. We train this model with  $\mathcal{L}_{KL}$ . Since both subnets make predictions on the same input feature maps, we assume that experts in each subnet are specialized in similar domains. A shared gating network further reduces model size, number of trainable parameters, and training time.

Table 4 states the results. None of the *DetectorMoE* models beats the baseline model. Although all models perform similarly independent of the training constraint, the hard constrained model seems to perform slightly better than the soft constrained models. We further observe only a slight performance drop for the model with a single gating network compared to 2 separate gating networks.

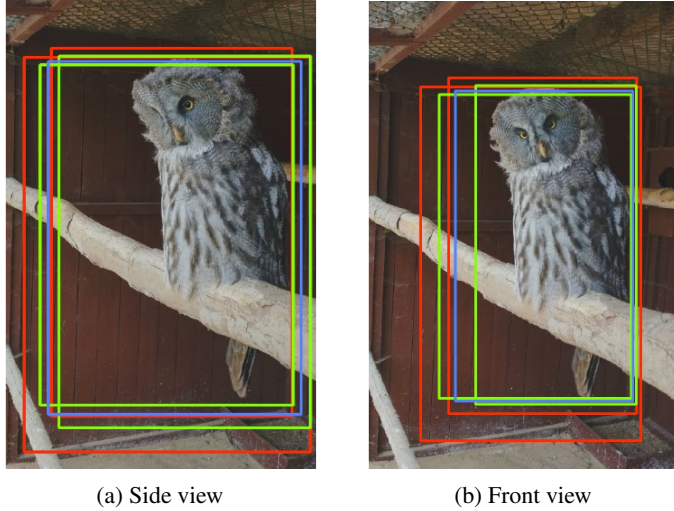
#### 4.2.3 Qualitative Analysis of Regressor MoE.

To gain insights into the weighting decisions of BBox regressor, we visualize different BBox predictions. Fig. 4 shows visualisation exemplary for *DetectorMoE-KL-4* for the same object from different angles. All 4 experts have problems estimating the precise object boundaries for atypical poses and situations. Predictions on objects with a clear front view vary less. The gating network is again able to choose eligible experts for the input in Fig. 4b. Hence, the gating network assigns about twice as much weight to the inferior expert than the most precise one. It underlines the fact that

<sup>3</sup> Available at <https://github.com/yhenon/pytorch-retinanet> (Apache License 2.0.)

Table 4: Object detection mAP (%) of MoE models on COCO test-dev2017

Model	mAP@[.5, .95]	mAP@.5
<i>Baseline</i>	35.0	52.5
<i>DetectorMoE-KL-4</i>	33.5	50.9
<i>DetectorMoE-Imp-4</i>	33.5	50.9
<i>DetectorMoE-Rel-4</i>	33.7	51.0
<i>DetectorMoE-KL-4 Single</i>	33.4	50.9
<i>DetectorMoE-KL-4 Conv4</i>	33.6	50.9
<i>DetectorMoE-Rel-4 Conv4</i>	33.6	50.9
<i>DetectorMoE-KL-4 Pretrained</i>	<b>35.1</b>	<b>52.7</b>
<i>DetectorMoE-Rel-4 Pretrained</i>	34.4	51.7
<i>DetectorMoE-KL-4 Conv 4 Pretrained</i>	<b>35.1</b>	52.6

Figure 4: BBox predictions of *DetectorMoE-KL-4* (blue) and its distinct experts (predictions of 2 active experts are green)

the gating network is not always able to pick the single best expert. Still, the inactive experts would both overestimate the bottom of the bounding box, while the selected experts both predict the bottom tightly. Further visualizations of BBox predictions can be found in the supplements.

#### 4.2.4 Pre-Trained Expert Networks.

Finally, we investigate the behavior of MoE models using pre-trained weights for expert networks. For this, we re-use baseline weights and add Gaussian noise to them to enable different expert specialization. Furthermore, we reduce the learning rate and the number of training epochs and set  $w_{kl} = 0.05$  since each expert is already able to detect objects reliably. For the hard constrained *DetectorMoE-Rel-4*, we keep  $m_{rel} = 0.3$  since it already allows the gating network to vary more between different experts.

In addition, we train *Conv4* models by only replacing the 4<sup>th</sup> convolutional layers in the regressor and classifier subnets with an MoE layer. We also use pre-trained weights for the whole model and add noise to the expert networks. Because the basic *DetectorMoE-KL-4* performs better for pre-trained weights than the hard constrained equivalent, we set  $w_{kl} = 0.05$ . We freeze the backbone weights and only update the regressor and classifier subnets. For comparison, we also train *Conv4* models without pre-trained weights (see Table 4).

Both *KL*-models with pre-trained weights outperform the baseline slightly in most metrics. Models with pre-trained weights outperform models trained from scratch. Soft-constrained models show larger improvements than hard-constrained ones.

Overall, using pre-trained weights increases the performance significantly compared to training from scratch, but obstructs expert specializations. Consequently, the decision-making process of the MoE model becomes less transparent

and interpretable. It seems to be a tradeoff between interpretability and expert specialization in the MoE architecture and performance of the overall model.

## 5 Conclusion

In this work, we showed how sparsely-gated MoE layers can be embedded into standard CNNs for computer vision tasks and presented soft and hard constraints to mitigate the dying expert problem. The proposed constraints tackle the problem from different angles and lead to different MoE behavior. Hard constraints result in a better overall performance and generalized experts, although the mean importance constraint is particularly prone to the dying experts problem. Soft constraints, on the other hand, lead to better expert specialization.

MoE embedding allowed us to increase the model capacity extensively while keeping an appropriate inference time by determining the number of active experts per forward pass. In our experiments both soft- and hard-constrained models achieved comparable test results, some MoE models even outperformed the baseline and showed accuracy improvements. The prediction performance of MoE models can be even further improved by increasing the number of active experts. This way, we can balance the trade-off between model accuracy and computational complexity with a single parameter. This helps in training models with many experts and parameters on powerful hardware and then scale the runtime complexity based on the deployment device.

Our results further showed that experts trained end-to-end without predefined dataset splits were still able to specialize in distinct subdomains. For image classification task, experts focused on specific class groups, whereas for object detection, they specialized on objects of distinct sizes.

## Acknowledgement

The research leading to these results is funded by the German Federal Ministry for Economic Affairs and Climate Action within the project “KI Absicherung“ (grant 19A19005W) and by KASTEL Security Research Labs. The authors would like to thank the consortium for the successful cooperation

## References

- [1] Robert A. Jacobs, Michael I. Jordan, Steven J. Nowlan, and Geoffrey E. Hinton. Adaptive mixtures of local experts. *Neural computation*, 3(1), 1991.
- [2] Noam Shazeer, Azalia Mirhoseini, Krzysztof Maziarz, Andy Davis, Quoc V. Le, Geoffrey E. Hinton, and Jeff Dean. Outrageously large neural networks: The sparsely-gated mixture-of-experts layer. In *Proceedings of the International Conference on Learning Representations (ICLR)*, 2017.
- [3] Emmanuel Bengio, Pierre-Luc Bacon, Joelle Pineau, and Doina Precup. Conditional computation in neural networks for faster models. *CoRR*, abs/1511.06297, 2015.
- [4] Dmitry Lepikhin, HyoukJoong Lee, Yuanzhong Xu, Dehao Chen, Orhan Firat, Yanping Huang, Maxim Krikun, Noam Shazeer, and Zhifeng Chen. Gshard: Scaling giant models with conditional computation and automatic sharding. In *Proceedings of the International Conference on Learning Representations (ICLR)*, 2021.
- [5] Samyam Rajbhandari, Conglong Li, Zhewei Yao, Minjia Zhang, Reza Yazdani Aminabadi, Ammar Ahmad Awan, Jeff Rasley, and Yuxiong He. Deepspeed-moe: Advancing mixture-of-experts inference and training to power next-generation AI scale. *CoRR*, abs/2201.05596, 2022.
- [6] Carlos Riquelme, Joan Puigcerver, Basil Mustafa, Maxim Neumann, Rodolphe Jenatton, André Susano Pinto, Daniel Keysers, and Neil Houlsby. Scaling vision with sparse mixture of experts. *CoRR*, abs/2106.05974, 2021.
- [7] Fuzhao Xue, Ziji Shi, Futao Wei, Yuxuan Lou, Yong Liu, and Yang You. Go wider instead of deeper. *CoRR*, abs/2107.11817, 2021.
- [8] David Eigen, Marc’Aurelio Ranzato, and Ilya Sutskever. Learning factored representations in a deep mixture of experts. In Yoshua Bengio and Yann LeCun, editors, *Proceedings of the International Conference on Learning Representations (ICLR)*, 2014.
- [9] Lu Lu, Yeonjong Shin, Yanhui Su, and George E. Karniadakis. Dying relu and initialization: Theory and numerical examples. *CoRR*, abs/1903.06733, 2019.
- [10] Alex Krizhevsky, Geoffrey Hinton, et al. Learning multiple layers of features from tiny images. 2009.

- [11] Kaiming He, Xiangyu Zhang, Shaoqing Ren, and Jian Sun. Deep residual learning for image recognition. In *Proceedings of the IEEE/CVF Conference on Computer Vision and Pattern Recognition (CVPR)*. IEEE, 2016.
- [12] Tsung-Yi Lin, Michael Maire, Serge J. Belongie, James Hays, Pietro Perona, Deva Ramanan, Piotr Dollár, and C. Lawrence Zitnick. Microsoft COCO: common objects in context. In David J. Fleet, Tomás Pajdla, Bernt Schiele, and Tinne Tuytelaars, editors, *Proceedings of the European Conference on Computer Vision (ECCV)*. Springer, 2014.
- [13] Tsung-Yi Lin, Priya Goyal, Ross B. Girshick, Kaiming He, and Piotr Dollár. Focal loss for dense object detection. In *Proceedings of the IEEE International Conference on Computer Vision (ICCV)*, pages 2999–3007. IEEE Computer Society, 2017.
- [14] Kaiming He, Xiangyu Zhang, Shaoqing Ren, and Jian Sun. Delving deep into rectifiers: Surpassing human-level performance on imagenet classification. In *Proceedings of the IEEE International Conference on Computer Vision (ICCV)*. IEEE, 2015.